Energy & Environmental Science

ROYAL SOCIETY OF CHEMISTRY

PAPER

Cite this: *Energy Environ. Sci.*, 2021, **14**, 5541

High efficiency deep red to yellow photochemical upconversion under solar irradiance†

Joseph K. Gallaher,[a] Katherine M. Wright,[b] Laszlo Frazer,[ac] Rowan W. MacQueen,[ad] Maxwell J. Crossley,[e] Felix N. Castellano[b] and Timothy W. Schmidt*[a]

Received 16th July 2021,
Accepted 9th September 2021

DOI: 10.1039/d1ee02197d

rsc.li/ees

The performance of a perylene monoimide annihilator is evaluated in a photochemical upconversion composition. It is found to perform up to five times better than the commonly employed rubrene annihilator at low excitation intensity, but suffers from a low annihilation singlet yield which hinders its performance under strong excitation. Upconversion action spectroscopy under broadband bias reveals that under one sun illumination, an upconversion composition employing the perylene monoimide utilizes more than 12% of the generated triplet states to generate emissive, excited singlet states. In a suitable medium, this composition could enhance the energy conversion efficiency of high band gap solar cells.

Broader context

Solar energy is abundant. Discovering ways to harvest solar energy efficiently are of particular interest. But, single-threshold solar cells, and emerging perovskite technologies in particular, do not harvest low energy photons. Photochemical upconversion by triplet fusion is a strategy to overcome this limitation by upconverting low energy photons from below to above the band gap of the solar cell. But, efficient upconversion in the relevant part of the spectrum at one-sun illumination has been elusive, in part due to a scarcity of high-performance triplet annihilators with low energy triplet states. In this paper we show that a perylene monoimide annihilator, when coupled to a far-red absorbing metalloporphyrin, can utilize up to 12% of generated triplet states in the upconversion process under one-sun illumination. The present composition is applicable to solar cells with band gaps above 1.85 eV, but with further sensitizer development could be pushed into the near infrared region of the spectrum.

Introduction

Solar energy is delivered to the Earth as a broadband spectrum, reaching the planet's surface with an intensity of about 1 kW m^{-2}. However, making efficient use of this energy presents certain challenges. A silicon solar cell does not make use of that part of the spectrum with wavelengths longer than 1100 nm, and at best can provide an open circuit voltage of about 750 mV.[1] These limitations cap the achievable energy conversion efficiency of a crystalline silicon solar cell to 29%,[2] and that of any single-junction semiconductor to 33.7% under the standard AM1.5G spectrum.[3–5]

To move beyond the single-junction limit requires more efficient use of the solar spectrum. There are several strategies to achieve this. Multi-junction cells hold records for energy conversion efficiencies,[1,6,7] using several band-gaps to sequentially harvest the solar spectrum from higher to lower photon energies. However, these devices are rather expensive, and are best suited to concentrator photovoltaic systems.[8] Other strategies to overcome the single-junction limit include multiple exciton generation[9] (including singlet fission[4,10–15]), intermediate band solar cells,[16–19] hot carrier solar cells,[20] and upconversion.[21,22]

Upconversion (UC) is a process whereby two or more lower energy photons are combined by a material to produce higher energy photons (Fig. 1). Detailed balance calculations show that a solar cell utilizing efficient UC is limited to about 43% energy conversion efficiency.[4] Under solar concentration this figure is lifted to in excess of 50%.[23]

[a] *ARC Centre of Excellence in Exciton Science, School of Chemistry, UNSW Sydney, NSW 2052, Australia. E-mail: timothy.schmidt@unsw.edu.au*
[b] *Department of Chemistry, North Carolina State University, Raleigh, NC 27695, USA*
[c] *ARC Centre of Excellence in Exciton Science, School of Chemistry, Monash University, Clayton, VIC 3800, Australia*
[d] *Department of Spins in Energy Conversion and Quantum Information Science, Helmholtz-Zentrum Berlin für Materialen und Energie GmbH, Berlin, Germany*
[e] *School of Chemistry, The University of Sydney, NSW 2006, Australia*

† Electronic supplementary information (ESI) available: Full details of the materials and sample preparation and optical spectroscopy methods. Additional figures. See DOI: 10.1039/d1ee02197d

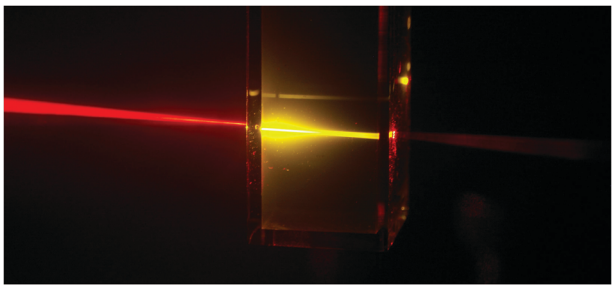

Fig. 1 Upconversion in action. Red light is absorbed by a bespoke porphyrin and the triplet energy is transferred to PMI or rubrene, which then undergoes triplet–triplet annihilation and emits higher energy, yellow light.

Experimental demonstrations of UC fall into two categories: rare-earth UC[24] and photochemical UC.[25,26] While both photochemical and rare-earth upconversion is applicable to silicon photovoltaics,[27,28] those cells which stand to gain the most from UC are those with higher band gaps,[23] which include many thin-film technologies as well as the emerging methylammonium lead halide perovskite solar cells.[29] These higher band gaps are best addressed with photochemical upconversion (PUC).[22,26]

In PUC, photons are harvested by sensitizer molecules which undergo rapid intersystem crossing to generate molecular triplet states (Fig. 2). In a well designed system, this triplet energy is rapidly transfered to annihilator molecules which can store the energy for hundreds of microseconds – long enough for two such triplet states to interact.[30] When two annihilator triplets

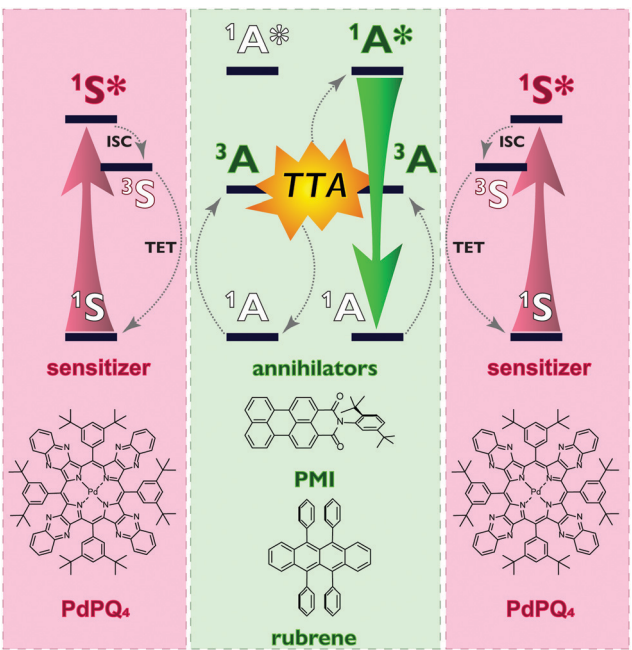

Fig. 2 The energy transfer scheme involved in photochemical upconversion. Large, solid arrows indicate photon absorption and emission events. Structures of molecules used in this study are shown at the bottom. ISC: intersystem crossing; TET: triplet energy transfer; TTA: triplet–triplet annihilation.

"annihilate", they ideally generate an excited singlet state which promptly results in a photon of higher energy than that originally absorbed. This process is also known as triplet fusion.[31] PUC has been intensively studied over the past decade and a half,[32–47] and has been applied to various photovoltaic and photocatalytic technologies.[31,48–54]

The most widely used annihilator molecule in PUC studies is diphenylanthracene, coupled with a platinum or palladium octaethylporphyrin sensitizer.[32,55–57] Such a combination can generate blue light from green light with a quantum yield of about 5% under one-sun conditions.[58] Other green-to-blue systems employing perylene were found to double this performance,[59–61] and the perylene annihilator stands as the record holder for upconversion efficiency. However, thin film photovoltaics exhibit absorption thresholds in the red and near-infrared regions of the spectrum, requiring sensitizers and annihilators with lower energy triplet states. One parameter in the road map to optimising the efficiency of solar photon upconversion is expanding the library of possible triplet-acceptors to find more effective annihilator species.[62]

In our demonstrations of upconversion applied to photovoltaics,[49–54] we have nearly exclusively used rubrene as the annihilator, and a palladium porphyrin with extended conjugation as the sensitizer. Rubrene is an intrinsically efficient annihilator, with two triplets generating a singlet with high probability,[38,39] but it diffuses slowly. We previously estimated its second order triplet–triplet annihilation rate constant at just 1×10^8 M^{-1} s^{-1},[38,39,63] more than an order of magnitude below the diffusion limit in typical solvents. This limits its efficency under one-sun pumping with available sensitizer materials. Nevertheless, we have achieved upconversion enhancements to current densities exceeding 4.5×10^{-3} mA cm^{-2} under one sun.[54] In order to increase this figure of merit,[64] we require an annihilator significantly more effective than rubrene.

In this contribution, we report a perylene monoimide (PMI) annihilator[65] which, when coupled to our bespoke porphyrin, generates excited singlet states with normalized state upconversion efficiency $\eta_{UCs} > 12\%$ under broadband, one-sun pumping.[66] At just 0.1 suns, η_{UCs} is >5%, five times that of rubrene. This significant improvement brings us a step closer to realising efficient photochemical upconversion for photovoltaics under low-intensity (sub)-solar conditions.

Methods

Sample preparation

All samples for optical spectroscopy were prepared under nitrogen atmosphere inside a glovebox, with an internal environment maintained at <0.5 ppm O_2. Full details of the materials and sample preparation can be found in the ESI.† Briefly, upconversion blends of PMI:$PdPQ_4$, and rubrene:$PdPQ_4$ were prepared by first preparing individual stock solutions of each component in anhydrous toluene. To make the upconversion blends an aliquot of annihilator stock solution (*i.e.*, PMI or rubrene) was added to an equal volume of $PdPQ_4$ stock solution, and stirred for 3 hours

to ensure mixing of the final solutions. In action spectra experiments, the PMI : $PdPQ_4$ blend had concentrations of 2.5 : 1 mM. The rubrene : $PdPQ_4$ blend had concentrations of 10 : 1 mM. The lower concentration of PMI was due to its lower solubility in toluene compared to rubrene, which limited the stock solution concentration. For relative external quantum yield experiments, both compositions were made at concentrations of 1 : 0.1 mM. Before removal from the glovebox, all samples were sealed under inert atmosphere using a custom quartz curvette with a 1 mm path length, fitted with a J-Young greaseless stopcock.

Optical spectroscopy

External quantum yield measurements were performed on a home-built setup. A 670 nm laser diode was used as the excitation source, and the laser output focused, providing an elliptical spot with dimensions of approximately 437 × 210 μm (measured to $1/e^2$) incident on the upconversion sample. Sample photoluminescence was collected parallel to the excitation axis using parabolic mirrors, filtered using a 650 nm short-pass filter to remove any residual excitation, and fibre-coupled into a high-resolution USB-spectrometer (Ocean Optics HR4000). The excitation light was attenuated using neutral density filters and a series of spectra were collected for a range of excitation powers affording a measure of external photon yield, and subsequent comparison of, rubrene:$PdPQ_4$ and PMI:$PdPQ_4$ blends over a range of excitation power densities.

Excitation-action spectra were collected according to our previously reported home built setup.[58,67] In this study the broadband bias beam (Energetiq LDLS EQ-1500) was filtered using a 650 nm long-pass filter to give resonant excitation with the Q-band structure of $PdPQ_4$ absorption (the upconverting region).[38,68]

Time-resolved photoluminescence spectroscopy was carried out using a 150 fs regeneratively amplified titanium-doped sapphire laser (Clark-MXR CPA 2210), operating at a repetition rate of 1 kHz and with a fundamental wavelength of 780 nm, and an optical parametric amplifier (Light Conversion TOPAS-C) to produce excitation pulses of either 532 or 670 nm. The luminescence spectra of samples were recorded as a function of time delay after laser excitation and collected with an intensified CCD camera (Princeton Instruments PI-MAX4) mounted to a spectrograph (Acton SP-2150i).

Results and discussion

Terminology

Because this manuscript deals extensively with the concept of upconversion efficiency, it is important to clearly lay out the terminology used. Recently, we published a viewpoint in which we made recommendations for the terminologies to be used in upconversion studies.[66] In it, we recommended that the symbol Φ only be used for quantum yields, and where the figure is doubled so that the maximum is unity, the symbol η is used. As such, while the maximum Φ_{TTA} is 0.5, the corresponding η_{TTA} is unity. A summary of relevant terms is given in Table 1.

Table 1 Definitions of important terms in photochemical upconversion[66]

Symbol	Meaning	Max.
$\#^1S^*$	# of excited singlet sensitizers	
$\#^3S^*$	# of excited triplet sensitizers	
$\#^1A^*$	# of excited singlet annihilators	
$\#^3A^*$	# of excited triplet annihilators	
$\#h\nu$	# of emitted photons	
#cp	# of reactive contact pairs	
$\Phi_{ISC} = \#^3S^*/\#^1S^*$	Intersystem crossing QY	1
$\Phi_{TET} = \#^3A^*/\#^3S^*$	Triplet energy transfer QY	1
$\Phi_{TTA} = \#^1A^*/\#^3A^*$	Triplet–triplet annihilation QY	0.5
$\Phi_F = \#h\nu/\#^1A^*$	Fluorescence QY	1
$\Phi_{UCs} = \Phi_{ISC}\Phi_{TET}\Phi_{TTA}$	Upconversion state QY	0.5
$\Phi_{cp} = \#cp/\#^3A^*$	Contact pair QY	0.5
$f = \#^1A^*/\#cp$	Annihilation singlet yield	1
$\eta_\alpha = 2\Phi_\alpha$	Normalized efficiency[a]	
k_1	$^3A^*$ 1st-order decay constant	
k_2	$^3A^*$ 2nd-order decay constant	

[a] α = TTA,UC_s,cp.

A comprehensive list of terms including those not relevant to the present study can be found in ref. 66.

Relative TTA-UC performance

The structures of the sensitizer and annihilator chromophores used in this study are shown in Fig. 2. The steady-state optical absorption and emission spectra of *N*-(2,5-di-tert-butylphenyl)-perylene-3,4-dicarboximide (PMI) and porphyrin $PdPQ_4$ are shown in Fig. 3. PMI has a large extinction coefficient (ε_{506nm} = 35 800 mol^{-1} dm^3 cm^{-1}), consistent with other perylene-monoimide 2derivatives. Following photoexcitation, strong photoluminescence is observed over the range of 500–600 nm, with near unity fluorescence quantum yield. As can be seen in Fig. 3, the wavelengths of PMI emission range between the absorption features of the porphyrin sensitizer ($PdPQ_4$); this is preferable in

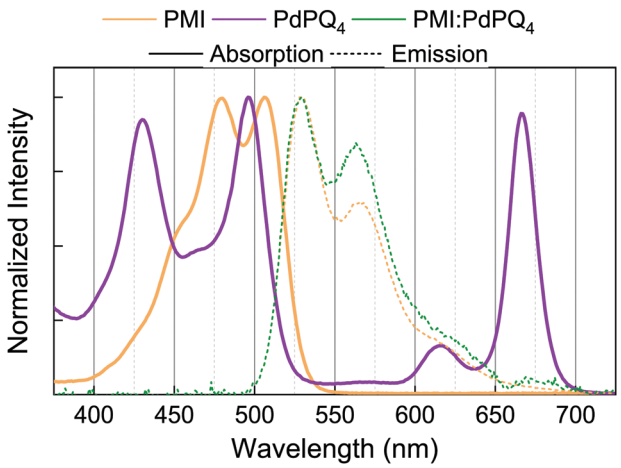

Fig. 3 Steady-state optical absorption (solid lines) and emission (dashed lines) spectra of PMI (7.7 mM), $PdPQ_4$ (2 mM), and a PMI:$PdPQ_4$ blend (2.5 : 1 molar ratio) in anhydrous toluene. The excitation wavelength for PMI was 505 nm, and 670 nm for the PMI:$PdPQ_4$ blend (within the absorption region of the porphyrin Q-band structure). The upconverted emission observed from the PMI:$PdPQ_4$ blend matches that of PMI emission, confirming TTA-UC.

photon upconversion processes in order to minimise reabsorption of upconverted photons, which would obviously negatively influence the yield of photons able to escape the upconverter sample matrix.

When paired together in a PMI:$PdPQ_4$ blend, PMI performs the role of the annihilator (triplet-acceptor), with $PdPQ_4$ as the sensitizer (triplet-donor). The optical absorption spectra of the PMI:$PdPQ_4$ blend is shown in the ESI.† Following photoexcitation of the PMI:$PdPQ_4$ blend at 670 nm (*i.e.*, within the absorption window of the porphyrin Q-band structure) an upconverted emission was detected between 500–650 nm, corresponding to fluorescence from PMI, confirming triplet–triplet annihilation upconversion (TTA-UC) of the pairing.

It is noted that the peaks corresponding to 0–0 and 0–1 transitions (529 and 563 nm, respectively) of PMI differ in relative peak intensity (*i.e.*, vibronic progression ratio) in neat PMI compared to the PMI:$PdPQ_4$ blend. This is likely a reabsorption effect due to the differing excitation depth profile brought about by direct excitation and sensitized triplet fusion.

Having confirmed TTA-UC occurs in the PMI:$PdPQ_4$ blend, the question at hand was how PMI performs as an annihilator, particularly, relative to other deep-red-to-yellow annihilator chromophores reported in the literature. In this regard, we turned to rubrene, a commonly used annihilator in upconversion blends, to act as a relative benchmark of efficiency when paired with the $PdPQ_4$ porphyrin sensitizer. The absorption and emission wavelengths of PMI and rubrene are substantially similar (see ESI†), which supports the use of rubrene as a relative comparison for upconversion efficiency.

To gain insight into the performance of PMI *versus* rubrene as annihilator species we probed the TTA-UC dynamics using time-resolved photoluminescence spectroscopy of each blend (see ESI†). Each sample was excited at 670 nm and the phosphorescence from $PdPQ_4$ triplets (800–900 nm), and the delayed-fluorescence resulting from TTA-UC of each annihilator species was measured. Both upconverter blends were at concentrations of 1 : 0.1 mM (annihilator : sensitizer) in anhydrous toluene.

Fig. 4A shows the wavelength-integrated photoluminescence (kinetics) of $PdPQ_4$ triplet phosphorescene when $PdPQ_4$ is paired with PMI and rubrene annihilators, integrated around 850 nm. For the PMI:$PdPQ_4$ blend, the phosphorescence has a lifetime of 780 (± 10) ns, which is a 150-fold decrease in phosphorescence lifetime compared to neat (pure) $PdPQ_4$ (125 ± 1 μs lifetime). Notably, the $PdPQ_4$ phosphorescence lifetime in the PMI:$PdPQ_4$ blend is significantly shorter than the rubrene:$PdPQ_4$ blend (2.9 ± 0.1 μs). The phosphorescence lifetime of $PdPQ_4$ triplets is indicative of the triplet-energy-transfer (TET) rate from sensitiser to annihilator. This implies that TET is more rapid from $PdPQ_4$ to PMI than to rubrene. However, in both cases the triplet energy transfer yield, Φ_{TET}, is essentially unity.

The time-resolved anti-Stokes delayed-fluorescence from each annihilator (integrated around 570 nm for PMI, and 580 nm for rubrene) are shown in Fig. 4B. The signatures are consistent with TTA-UC processes, namely, an anti-Stokes

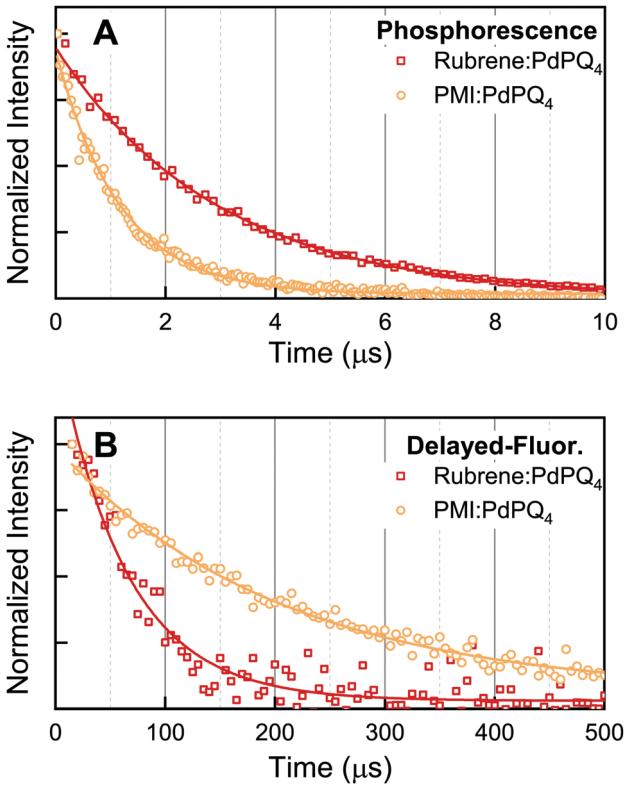

Fig. 4 Time-resolved photoluminescence (TRPL) of PMI:$PdPQ_4$ and rubrene:$PdPQ_4$ blends following photoexcitation at 670 nm, showing the kinetics at of (A) phosphorescence from $PdPQ_4$ (integrated around 850 nm) and (B) delayed-fluorescence which results from emission from PMI (integrated around 570 nm) or rubrene (integrated around 580 nm). The solid lines are mono-exponential fits to the experimental data. Both upconverter blends were at a concentration of 1 : 0.1 mM ratio (annihilator:sensitizer) in anhydrous toluene.

photoluminescence from annihilator singlet states on a delayed timescale (*i.e.*, delayed-fluorescence).

The kinetics of triplet decay is given by[30]

$$\frac{d[T]}{dt} = -k_1[T] - k_2[T]^2 \quad (1)$$

with the rate of generation of upconverted photons given by

$$\frac{d[h\nu]}{dt} = f\frac{k_2[T]^2}{2}\Phi_F \quad (2)$$

where f accounts for spin-statistical factors and Φ_F is the fluorescence quantum yield. Where $k_2[T] \ll k_1$, the decay of [T] is dominated by first order kinetics and approaches exponential behaviour with rate constant k_1. Because the upconverted light depends on the square of the triplet concentration, it decays with twice the rate constant,

$$\frac{d[h\nu]}{dt} \propto \exp(-2k_1 t). \quad (3)$$

The kinetics of delayed-fluorescence of the PMI:$PdPQ_4$ blend are well represented by a monoexponential decay, with a fitted lifetime of 203 ± 10 μs. As seen in Fig. 4B, the delayed-fluorescence lifetime of PMI (in the PMI:$PdPQ_4$ blend) is

Table 2 Derived values from modelling excitation-action spectra

	k_1 (s^{-1})	k_2 (M^{-1} s^{-1})	f
PMI	$2.46(12) \times 10^3$	3.0×10^9	0.23
Rubrene	$8.1(5) \times 10^3$	9.5×10^8	~1

significantly longer than observed for rubrene in the rubrene:$PdPQ_4$ blend, which has a lifetime of 62 ± 4 μs. These measurements provide estimates of k_1 for each species, but should be considered a lower bound where sensitizer concentrations are higher (Table 2).[69]

The TTA-UC phosphorescence dynamics are consistent with a lower k_1 for PMI, which augurs well for upconversion efficiency. As will be discussed in further detail below, the comparison of PMI and rubrene is ideally poised to provide insight into what effect the annihilation rate constant (k_2) *vis-a-vis* a poorer annihilation singlet-yield (f) of an annihilator species may have on the overall TTA-UC process.

Exploiting TTA-UC in a device context relies on maximising the number of photons being emitted back into a solar cell it is. In this regard, when considering the efficiency of UC, it is pertinent to give attention to the number of upconverted photons which are able to escape at TTA-UC sample matrix. With this in mind, and as a first approximation of the relative performance (proxy of efficiency) of the upconvertor blends, we performed simple relative external quantum yield measurements for a direct comparison of PMI and rubrene. A monochromatic excitation source (670 nm laser diode) was used to excite each TTA-UC blend and a portion of the delayed-PL from the sample was collected on a USB-spectrometer (see ESI† for further details and spectra).

Fig. 5 shows a double-logarithmic plot of integrated delayed-PL intensity for PMI:$PdPQ_4$ and rubrene:$PdPQ_4$ blends as a function of excitation power. In addition to detector and background corrections (see ESI†), the PL intensity has been normalised and rescaled onto a relative PL intensity scale in order to directly compare the PL output. For each spectrum, in both the PMI and rubrene series, the spectra have been area-normalised to that of the rubrene:$PdPQ_4$ delayed-PL at the highest excitation power. Subsequently, the PMI:$PdPQ_4$ series has been re-scaled by the ratio of the area of rubrene and PMI at highest power, allowing a relative comparison in collected upconverted photons of the two upconverter blends.

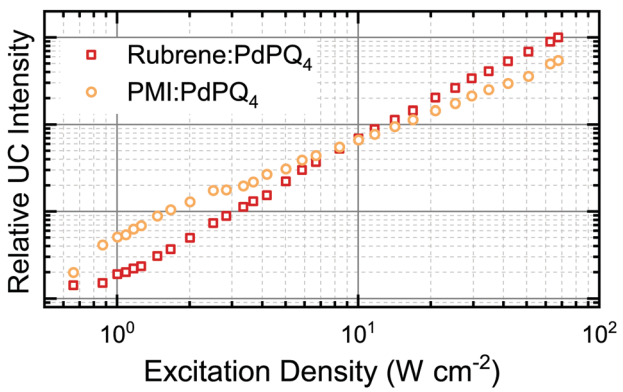

Fig. 5 Integrated steady-state upconversion intensity for PMI:$PdPQ_4$ and rubrene:$PdPQ_4$ blends as a function of excitation power, from external quantum yield measurements. Both upconverter blends were excited at 670 nm. The intensity axis has rescaled to allow for a relative comparison, as described in the text.

At first glance, it is clear that at low excitation powers (<10 W cm^{-2}) the number of photons escaping the upconvertor matrix (*i.e.*, the relative external PL yield) is greater for PMI than rubrene. However, at higher excitation powers the PL intensity from PMI levels off, approaching a slope of 1 (see Fig. S12, ESI†), and the rubrene blend has a greater number of escaping external photons. As a result there is a cross-over in relative PL intensity at an excitation density threshold of approximately 10 W cm^{-2}, at this sensitizer concentration. Since the sensitizer and its concentration is the same in both blends, and the only difference is the annihilator, this result suggests a difference in TTA-UC efficiency (Φ_{UC}) which, as discussed in more detail below, can be ascribed to differences in first- and second-order rate constants (*i.e.*, k_1 and k_2, respectively) and/or the annihilation singlet-yield of the annihilator species, f.[23,66,68]

Modelling TTA-UC efficiency

Gauging the efficiency of an efficient upconvertor under simulated solar pumping is a non-trivial task. Simple external quantum efficiency measurements, while useful, will tend to underestimate the intrinsic efficiency of the TTA process without accounting for reabsorption effects. In previous work, we reported a method to measure the efficiency with which triplet states generate excited singlet states in an optically dense composition,[67] a technique referred to herein as excitation-action spectroscopy. Briefly, annihilator fluorescence is measured at a particular wavelength as the linear response of the upconversion composition to a chopped, monochromated probe beam, using lock-in amplification. Since the linear response of a quadratic process is zero, the upconvertor is placed under a continuous pump, exciting sensitizer molecules at a rate comparable to solar excitation.

Fig. 6 shows the excitation-action spectra of the PMI:$PdPQ_4$ (Fig. 6A) and rubrene:$PdPQ_4$ (Fig. 6B) blends. The spectral features of the excitation spectra are characterised by absorption features from the sensitizer porphyrin (600–700 nm), and the 0–0 band of the corresponding annihilator (<550 nm). The plots have been normalized, with the intensity of the annihilator excitation feature set to unity.

Roughly speaking, since the plots are a measure of the linear response of upconverted light to a weak probe, the state upconversion quantum yield Φ_{UCs} can be gauged from the intensity of the sensitizer peak (with the annihilator peak set to unity). To arrive at a more accurate figure requires detailed modelling of the experiment.

In our previous work, we modelled upconversion action spectra using the assumption that at a depth z in the upconvertor the concentration of annihilator triplet states is in steady-state, thereby yielding the rate equation of the following

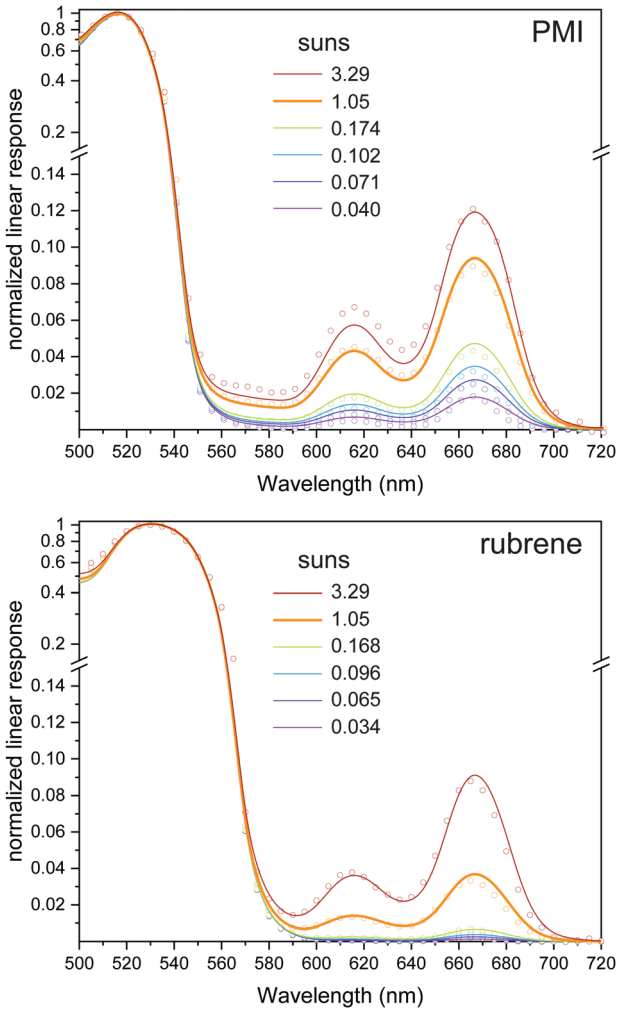

Fig. 6 Excitation-action spectra (symbols) of PQ_4Pd sensitized upconvertors with PMI (top) and rubrene (bottom) annihilator. The solid lines represent fits to the experimental data using the broadband bias model, as described in the text. The fits to 1.05-sun data are plotted as thick lines.

general form:

$$\frac{\mathrm{d}[T]_z}{\mathrm{d}t} = 0 = k_\phi(z)[\mathrm{S}] - k_1[\mathrm{T}]_z - k_2[\mathrm{T}]_z{}^2. \quad (4)$$

where $[\mathrm{T}]_z$ is the concentration of annihilator triplet states at depth z, [S] is the concentration of sensitizers, $k_\phi(z)$ is the excitation rate of the sensitizer, and k_1 and k_2 are the first and second-order annihilator triplet decay constants, respectively.

This assumption allowed modelling of the upconversion excitation-action spectra to quantitatively determine TTA efficiency by taking into account the reabsorption of emitted light by both the sensitizer and the annihilator, but without requiring knowledge of the fluorescence quantum yield. The action spectrum includes the direct excitation of the annihilator, so the measurement is internally calibrated. However, in our previous work, it was assumed that the bias pump was monochromatic and that the upconvertor remained, at all times, in the quadratic regime. In this work it was necessary to explicitly take account of broadband pumping. Thus, the excitation-action spectra were modelled using eqn (5)–(7).

$$\sigma(\lambda) = A \times \left(\frac{\alpha_\mathrm{p}^\mathrm{e}(\lambda)}{\alpha_\mathrm{p}(\lambda) + \alpha_\mathrm{PL}} + \int_0^\infty \mathrm{d}z f \Phi_\mathrm{cp}(z) \alpha_\mathrm{p}^\mathrm{s}(\lambda) \mathrm{e}^{-(\alpha_\mathrm{p}(\lambda)+\alpha_\mathrm{PL})z} \right) \quad (5)$$

and

$$\Phi_\mathrm{cp}(z) = \frac{1}{2} \frac{k_2[\mathrm{T}]_z}{k_2[\mathrm{T}]_z + k_1} \quad (6)$$

$$[\mathrm{T}]_z = \frac{-k_1 + \sqrt{k_1{}^2 + 4k_2 k_\phi(z)[\mathrm{S}]}}{2k_2} \quad (7)$$

The parameter A is an experimental scale factor, and the α terms are the (natural) extinction coefficients (with inverse dimension of length) of the upconversion blend at the probe wavelength (p) and photoluminescence detection wavelength (PL) of the annihilator (e) and the sensitizer (s). Further, f is the annihilation singlet-yield which accounts for the probability that the annihilation event of a pair of triplets yields the desired singlet. The function $\Phi_\mathrm{cp}(z)$ accounts for the effect of the change in triplet concentration ($[\mathrm{T}]_z$) as a function of depth (z) on the probability of second-order decay events due to contact pair formation.

The rate constant for the excitation rate of the sensitizer, $k_\phi(z)$, as a function of depth, z, may be determined by

$$k_\phi(z)[\mathrm{S}] = \int \mathrm{d}\lambda \mathscr{E}_\mathrm{bias}^\lambda(\lambda) \alpha_\mathrm{s}(\lambda) \exp(-\alpha(\lambda)z) \quad (8)$$

where $\mathscr{E}_\mathrm{bias}^\lambda(\lambda)$ is the spectral photon flux of the bias source, with units of photons per cm^2 per nm per s, having a known spectrum and spot size for each excitation condition.

As shown in Fig. 6 the shape of the excitation-action spectra are well reproduced by the above model (solid lines). Table 2 shows the parameters f and k_2 for each annihilator in the $PdPQ_4$ sensitised upconvertor blends resulting from the optimised fits (k_1 values were taken from the fits in Fig. 4). These derived values show that PMI has a lower f value, but a larger second order rate-constant than rubrene. This is notable as we have previously reported the potential impact that an increase in k_2 may have on the efficiency of an upconverter, calculating that 2-orders of magnitude increase in k_2 would provide a photon upconverter with efficiency 6-fold greater than a proposed threshold for device relevance.[62]

The relative performance of PMI and rubrene as an annihilator species in TTA-UC can be gauged by plotting

$$\eta_{\mathrm{UC_s}} = f \frac{k_2[\mathrm{T}]_0}{k_2[\mathrm{T}]_0 + k_1} \quad (9)$$

as a function of the bias intensity. This is a measure of the efficiency with which excited state annihilators are generated by excitation of the sensitizer at the front of the cuvette. As the light is extinguished as it penetrates the cuvette, this quantity naturally declines.

Fig. 7 shows the determined TTA-UC efficiencies as a function of bias intensity, measured in sun equivalence, for each blend. Immediately observed is that PMI is the more efficient

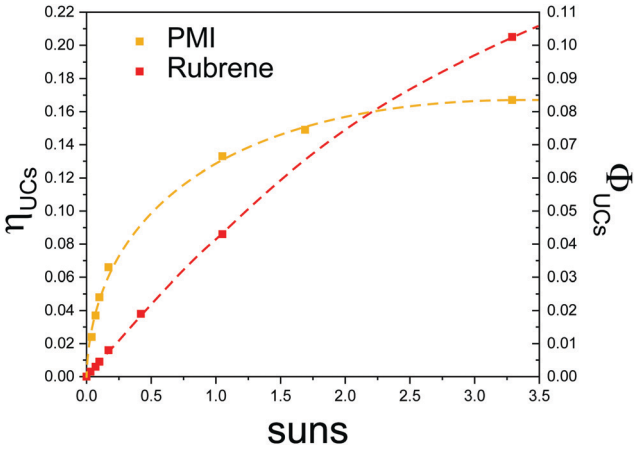

Fig. 7 (Normalized, left axis) upconversion state efficiencies for the PQ_4Pd sensitized upconvertors as a function of the bias intensity (in sun equivalence). The dashed lines are to guide the eye.

annihilator species at low bias intensity, but levels off and is overtaken in efficiency at higher bias intensity by rubrene. This is consistent with the trend observed in the external PL yield measurements (see above). Moreover, the modelled normalized state UC efficiency (η_{UCs}) for PMI, at just 0.1 suns, is 4.8%, which is five-times greater than that of rubrene. Further, at the literature benchmark value of one-sun equivalent excitation PMI achieves >12% normalized efficiency (>6% upconversion state quantum yield). As noted above, as the bias intensity increases η_{UCs} levels off earlier for PMI owing to its low f. In contrast, there is only a small levelling off for rubrene observed over the bias intensities probed, showing once more the cross-over in performance metric between the PMI and rubrene.

As seen from eqn (9), it follows that differences in the observed TTA efficiency can be attributed to differences in f, k_1, and k_2. One first observation is that the higher 'ceiling' of TTA-UC efficiency for rubrene would imply that rubrene has a greater annihilation singlet yield (f) compared to PMI.[68] Previously, we reported an f value for rubrene of about 0.6.[39] This was based on estimated excited state yields and the proportion of second-order decay, as gauged from kinetic traces. The excited state yields were determined from a front-face experiment comparing the yield of prompt and delayed fluorescence from rubrene in an upconversion composition.[38] The details of self-absorption were not considered. The discrepancy between the value obtained from modelling action spectra, and those from our previous published results warrants further investigation.

As will be discussed in further detail below, the present comparison of PMI and rubrene is ideally poised to provide insight into the effect of annihilation rate constant (k_2) *versus* a poorer annihilation singlet-yield (f) of an annihilator species on the TTA-UC efficiency.

TTA-UC efficiency battle: annihilator k_2 *vs.* f

At low excitation rates, the second order decay of annihilator triplets may be ignored and the triplet concentration is given by $[T] = k_\phi[S]/k_1$. From Eqn 2, we see that

$$\left.\frac{d[h\nu]}{dt}\right|_{low} = \frac{1}{2} f k_2 \left(\frac{k_\phi[S]}{k_1}\right)^2 \Phi_F \quad (10)$$

For high excitation rates, where the second order decay dominates, $[T] = \sqrt{k_\phi[S]/k_2}$, and

$$\left.\frac{d[h\nu]}{dt}\right|_{high} = \frac{1}{2} f k_\phi[S] \Phi_F \quad (11)$$

This change from quadratic to linear behaviour is often used to diagnose the upconversion threshold intensity, where the decay due to the first and second order processes are equal.[70–72]

Given the same sensitizer concentration and low excitation intensity, the rate at which excited singlet annihilators are generated is governed by $fk_2/{k_1}^2$. This quantity is fit to 114 s/M for PMI, but only 14 s M^{-1} for rubrene, and thus we can expect approximately 8 times as much upconverted light from a PMI composition than rubrene at low intensity (both $\Phi_F \sim 1$). The ratio of slopes at low intensity in Fig. 7 is 6.6. But, in Fig. 5, the ratio of upconverted light in the low intensity regime is a little more than double. Nevertheless, despite a lower f value, PMI performs better than rubrene at low intensities due in a large part to its lower first order rate of triplet decay, k_1. Its higher apparent k_2 value also contributes. This may be rationalised by the larger molecular size and steric hindrance of rubrene, compared to PMI, negatively influencing k_2. For example, size and steric-bulk could reduce the mobility of rubrene (annihilator) and molecular contact during possible TET collision events.[73]

In the high intensity limit, only f matters. Since PMI has a rather low f value, it reaches its efficiency and rubene overtakes at higher intensities. The question at hand is what effect this has on the realization of photon upconversion being applied to photovoltaic applications.

The champion annihilator is perylene itself. It was shown by Hoseinkhani *et al.* to exhibit an f of unity, and excellent sub-solar upconversion performance when coupled with palladium tetraphenyltetrabenzoporphyrin.[59] At one sun, an external upconversion quantum yield exceeding 10% was obtained, with about 3% being obtained at 0.1 suns. Although perylene-based annihilators have been used in some of the most efficient TTA-UC systems,[31,59,74] a potential drawback of perylene is a high inclination to aggregate and the formation of excimers (excited-state dimers), which commonly have a high rate of non-radiative decay.[75] The formation of dark-states such as excimers would, obviously, negatively impact the overall TTA-UC efficiency. However, we found no evidence of excimer formation in the present work.

The performance of PMI presented here shows that a higher annihilation rate constant, k_2, and lower triplet decay rate, k_1, of an annihilator can yield more efficient TTA-UC at low sun illumination, but a poor annihilation singlet yield, f, causes a reduced maximum efficiency achievable at high sun excitation. From benchmarking PMI against rubrene, we can outlay some

important design considerations for the road map to realising efficient photochemical upconversion for photovoltaics.

It is proposed that the dominant inherent characteristic of the annihilator that should be the centre of attention depends on the excitation conditions. If the target is for the greatest maximum efficiency in high-intensity situations, then any losses in overall TTA-UC efficiency caused a poor second-order rate constant, k_2, may be 'remedied by having a relatively high annihilation singlet yield, f.

On the other hand, in the search for efficient TTA-UC systems for use in applications with low-intensity illumination the annihilation rate constant, k_2, and the triplet decay rate (squared) appear to dominate the overall TTA-UC efficiency. Thus, at sub-solar intensities the design of an effective annihilator molecule should prioritize triplet lifetime, as well as factors contributing to maximising the diffusion of annihilators.

While the present study was undertaken exclusively in solutions, the principles outlayed here also apply to solid state upconvertors. Indeed, quasi-solid state materials may yet have a role to play in photovoltaics.[56,76]

Conclusions

We have characterized a perylene monoimide (PMI) derivative as an upconverting annihilator, comparing it to the commonly used rubrene. Using a variety of spectroscopies, we have established that it performs very well under low photon flux, when coupled with the $PdPQ_4$ sensitizer, owing to a low triplet decay rate and a higher triplet–triplet annihilation rate than rubrene. Yet, it suffers from a poor anihilation singlet yield, f, with only 23% of excitonically reactive contact pairs generating the excited singlet state. Under solar irradiance, our composition achieved over 6% upconversion state quantum yield, Φ_{UCs} which is 12% of the maximum achievable, η_{UCs}. The comparison between PMI and rubrene underlines that an annihilator that performs well at low excitation intensities, does not necessarily perform well at higher intensities, and *vice-versa*.

Author contributions

J. K. G., L. F. and R. W. M. performed the experiments. T. W. S. and F. N. C. conceived the study. J. K. G. and T. W. S. analysed the data and wrote the manuscript. M. J. C. designed and provided the sensitizer material. F. N. C. designed, and K. M. W. synthesised the PMI material.

Conflicts of interest

There are no conflicts of interest to declare.

Acknowledgements

This work was supported by the Australian Research Council (Centre of Excellence in Exciton Science CE170100026). T. W. S. also acknowledges the support of the Australian Research Council for a Future Fellowship (FT130100177). The work at NC State was supported by the U.S. Department of Energy, Office of Science, Office of Basic Energy Sciences, under Award No. DE-SC0011979.

References

1 M. A. Green, K. Emery, Y. Hishikawa, W. Warta and E. D. Dunlop, Solar cell efficiency tables (version 47), *Prog. Photovoltaics*, 2016, **24**, 3–11, PIP-15-272.
2 M. J. Kerr, P. Campbell and A. Cuevas, Limetime and Efficiency Limits of Crystalline Silicon Solar Cells, Proc. 29th IEEE PVSC 2002, pp. 438–441.
3 W. Shockley and H. J. Queisser, Detailed Balance Limit of Efficiency of P-N Junction Solar Cells, *J. Appl. Phys.*, 1961, **32**, 510–519.
4 M. J. Y. Tayebjee, D. R. McCamey and T. W. Schmidt, Beyond Shockley–Queisser: Molecular Approaches to High-Efficiency Photovoltaics. The, *J. Phys. Chem. Lett.*, 2015, **6**, 2367–2378.
5 B. Ehrler, E. M. Hutter and J. J. Berry, The Complicated Morality of Named Inventions, *ACS Energy Lett.*, 2021, **6**, 565–567.
6 P. T. Chiu, D. L. Law, R. L. Woo, S. Singer, W. D. Hong, A. Zakaria, J. C. Boisvert, S. Mesropian, R. R. King and N. H. Karam, Continued progress on direct bonded 5J space and terrestrial cells, Proc. 40th IEEE PVSC, 2014.
7 M. A. Steiner, R. M. France, J. Buencuerpo, J. F. Geisz, M. P. Nielsen, A. Pusch, W. J. Olavarria, M. Young and N. J. Ekins-Daukes, High Efficiency Inverted GaAs and GaInP/GaAs Solar Cells With Strain-Balanced GaInAs/GaAsP Quantum Wells, *Adv. Energy Mater.*, 2021, **11**, 2002874.
8 Fraunhofer Institute for Solar Energy Systems ISE, New world record for solar cell efficiency at 46%, Press Release, 26 2014.
9 M. C. Hanna and A. J. Nozik, Solar Conversion Efficiency of Photovoltaic and Photoelectrolysis Cells With Carrier Multiplication Absorbers, *J. Appl. Phys.*, 2006, **100**, 074510.
10 D. N. Congreve, J. Lee, N. J. Thompson, E. Hontz, S. R. Yost, P. D. Reusswig, M. E. Bahlke and S. Reineke, Van Voorhis, T.; Baldo, M. A. External Quantum Efficiency Above 100% in a Singlet-Exciton-Fission–Based Organic Photovoltaic Cell, *Science*, 2013, **340**, 334–337.
11 B. Ehrler, K. P. Musselman, M. L. Bohm, R. H. Friend and N. C. Greenham, Hybrid Pentacene/a-Silicon Solar Cells Utilizing Multiple Carrier Generation via Singlet Exciton Fission, *Appl. Phys. Lett.*, 2012, **101**, 153507.
12 M. J. Y. Tayebjee, A. A. Gray-Weale and T. W. Schmidt, Thermodynamic Limit of Exciton Fission Solar Cell Efficiency, *J. Phys. Chem. Lett.*, 2012, **3**, 2749–2754.
13 M. Einzinger, T. Wu, J. F. Kompalla, H. L. Smith, C. F. Perkinson, L. Nienhaus, S. Wieghold, D. N. Congreve, A. Kahn, M. G. Bawendi and M. A. Baldo, Sensitization of silicon by singlet exciton fission in tetracene, *Nature*, 2019, **571**, 90–94.

14 R. W. MacQueen, M. Liebhaber, J. Niederhausen, M. Mews, C. Gersmann, S. Jäckle, K. Jäger, M. J. Y. Tayebjee, T. W. Schmidt, B. Rech and K. Lips, Crystalline silicon solar cells with tetracene interlayers: the path to silicon-singlet fission heterojunction devices, *Mater. Horiz.*, 2018, **5**, 1065–1075.

15 A. Rao and R. H. Friend, Harnessing singlet exciton fission to break the Shockley–Queisser limit, *Nat. Rev. Mater.*, 2017, **2**, 17063.

16 A. Luque and A. Martí, Increasing the Efficiency of Ideal Solar Cells by Photon Induced Transitions at Intermediate Levels, *Phys. Rev. Lett.*, 1997, **78**, 5014.

17 N. J. Ekins-Daukes and T. W. Schmidt, A Molecular Approach to the Intermediate Band Solar Cell: The Symmetric Case, *Appl. Phys. Lett.*, 2008, **93**, 063507.

18 C. Simpson, T. M. Clarke, R. W. MacQueen, Y. Y. Cheng, A. J. Trevitt, A. J. Mozer, P. Wagner, T. W. Schmidt and A. Nattestad, An intermediate band dye-sensitised solar cell using triplet-triplet annihilation, *Phys. Chem. Chem. Phys.*, 2015, **17**, 24826–24830.

19 S. P. Hill, T. Dilbeck, E. Baduell and K. Hanson, Integrated Photon Upconversion Solar Cell via Molecular Self-Assembled Bilayers, *ACS Energy Lett.*, 2016, **1**, 3–8.

20 R. T. Ross and A. J. Nozik, Efficiency of hot-carrier solar energy converters, *J. Appl. Phys.*, 1982, **53**, 3813–3818.

21 T. Trupke, M. A. Green and P. Wurfel, Improving Solar Cell Efficiencies by up-conversion of Sub-Band-Gap Light, *J. Appl. Phys.*, 2002, **92**, 4117–4122.

22 T. F. Schulze and T. W. Schmidt, Photochemical Upconversion: Present Status and Prospects for its Application to Solar Energy Conversion, *Energy Environ. Sci.*, 2015, **8**, 103–125.

23 T. W. Schmidt and M. J. Y. Tayebjee, in *Comprehensive Renewable Energy*, Sayigh, A., ed., Elsevier, Oxford, 2012, pp 533–548.

24 F. Auzel, Upconversion and anti-Stokes processes with f and d ions in solids, *Chem. Rev.*, 2004, **104**, 139–173.

25 C. A. Parker and C. G. Hatchard, Sensitised Anti-Stokes Delayed Fluorescence, *Proc. Chem. Soc.*, 1962, 386–387.

26 T. N. Singh-Rachford and F. N. Castellano, Photon upconversion based on sensitized triplet-triplet annihilation, *Coordin. Chem. Rev.*, 2010, **254**, 2560–2573.

27 J. Goldschmidt, S. Fischer, B. Herter, B. Fröhlich, K. Krämer, B. Richards, A. Ivaturi, S. MacDougall, J. M. Hueso, E. Favilla and M. Tonelli, Record efficient upconverter solar cell devices, Proc. EU PVSEC, 2014, p. 1AP.1.2.

28 E. M. Gholizadeh, S. K. K. Prasad, Z. L. Teh, T. Ishwara, S. Norman, A. J. Petty II, J. H. Cole, S. Cheong, R. D. Tilley, J. E. Anthony, S. Huang and T. W. Schmidt, Photochemical upconversion of near-infrared light from below the silicon bandgap, *Nat. Photonics*, 2020, **14**, 585–590.

29 M. A. Green, A. Ho-Baillie and H. J. Snaith, The Emergence of Perovskite Solar Cells, *Nat. Photonics*, 2014, **8**, 506–514.

30 T. W. Schmidt and F. N. Castellano, Photochemical Upconversion: The Primacy of Kinetics. The, *J. Phys. Chem. Lett.*, 2014, **5**, 4062–4072.

31 B. D. Ravetz, A. B. Pun, E. M. Churchill, D. N. Congreve, T. Rovis and L. M. Campos, Photoredox catalysis using infrared light via triplet fusion upconversion, *Nature*, 2019, **565**, 343–346.

32 R. R. Islangulov, D. V. Kozlov and F. N. Castellano, Low power upconversion using MLCT sensitizers, *Chem. Commun.*, 2005, 3776–3778.

33 S. Baluschev, P. Keivanidis, G. Wegner, J. Jacob, A. Grimsdale, K. Müllen, T. Miteva, A. Yasuda and G. Nelles, Upconversion photoluminescence in poly (laddertype-pentaphenylene) doped with metal (II)-octaethyl porphyrins, *Appl. Phys. Lett.*, 2005, **86**, 061904.

34 T. N. Singh-Rachford and F. N. Castellano, Pd(II) Phthalocyanine-Sensitized Triplet-Triplet Annihilation from Rubrene, *J. Phys. Chem. A*, 2008, **112**, 3550–3556.

35 T. N. Singh-Rachford, A. Haefele, R. Ziessel and F. N. Castellano, Boron Dipyrromethene Chromophores: Next Generation Triplet Acceptors/Annihilators for Low Power Upconversion Schemes, *J. Am. Chem. Soc.*, 2008, **130**, 16164.

36 A. Monguzzi, R. Tubino and F. Meinardi, Multicomponent polymeric film for red to green low power sensitized upconversion, *J. Phys. Chem. A*, 2009, **113**, 1171–1174.

37 Y. Y. Cheng, B. Fückel, T. Khoury, R. G. C. R. Clady, N. J. Ekins-Daukes, M. J. Crossley and T. W. Schmidt, Entropically driven photochemical upconversion, *J. Phys. Chem. A*, 2011, **115**, 1047–1053.

38 Y. Cheng, T. Khoury, R. G. C. R. Clady, M. J. Y. Tayebjee, N. J. Ekins-Daukes, M. J. Crossley and T. W. Schmidt, On the efficiency limit of triplet-triplet annihilation for photochemical upconversion, *Phys. Chem. Chem. Phys.*, 2010, **12**, 66–71.

39 Y. Cheng, B. Fückel, T. Khoury, R. G. C. R. Clady, M. J. Y. Tayebjee, N. J. Ekins-Daukes, M. J. Crossley and T. W. Schmidt, Kinetic Analysis of Photochemical Upconversion by Triplet-Triplet Annihilation: Beyond Any Spin Statistical Limit, *J. Phys. Chem. Lett.*, 2010, **1**, 1795–1799.

40 Y. Murakami, Photochemical photon upconverters with ionic liquids, *ChemPhysLett*, 2011, **516**, 56–61.

41 V. Jankus, E. W. Snedden, D. W. Bright, V. L. Whittle, J. A. G. Williams and A. Monkman, Energy Upconversion via Triplet Fusion in Super Yellow PPV Films Doped with Palladium Tetraphenyltetrabenzoporphyrin: a Comprehensive Investigation of Exciton Dynamics, *Adv. Funct. Mater.*, 2013, **23**, 384–393.

42 V. Gray, D. Dzebo, M. Abrahamsson, B. Albinsson and K. Moth-Poulsen, Triplet-triplet annihilation photon-upconversion: towards solar energy applications, *Phys. Chem. Chem. Phys.*, 2014, **16**, 10345–10352.

43 Z. Huang, X. Li, M. Mahboub, K. M. Hanson, V. M. Nichols, H. Le, M. L. Tang and C. J. Bardeen, Hybrid Molecule–Nanocrystal Photon Upconversion Across the Visible and Near-Infrared, *Nano Lett.*, 2015, **15**, 5552–5557.

44 C. Mongin, S. Garakyaraghi, N. Razgoniaeva, M. Zamkov and F. N. Castellano, Direct observation of triplet energy transfer from semiconductor nanocrystals, *Science*, 2016, **351**, 369–372.

45 Y. C. Simon and C. Weder, Low-power photon upconversion through triplet–triplet annihilation in polymers, *J. Mater. Chem.*, 2012, **22**, 20817.

46 K. Okumura, K. Mase, N. Yanai and N. Kimizuka, Employing Core-Shell Quantum Dots as Triplet Sensitizers for Photon Upconversion, *Chem. – Eur. J.*, 2016, **22**, 7721–7726.

47 S. Amemori, Y. Sasaki, N. Yanai and N. Kimizuka, Near-Infrared-to-Visible Photon Upconversion Sensitized by a Metal Complex with Spin-Forbidden yet Strong S0–T1 Absorption, *J. Am. Chem. Soc.*, 2016, **138**(28), 8702–8705.

48 R. S. Khnayzer, J. Blumhoff, J. A. Harrington, A. Haefele, F. Deng and F. N. Castellano, Upconversion-powered photoelectrochemistry, *Chem. Commun.*, 2012, **48**, 209–211.

49 Y. Y. Cheng, B. Fückel, R. W. MacQueen, T. Khoury, R. G. C. R. Clady, T. F. Schulze, N. J. Ekins-Daukes, M. J. Crossley, B. Stannowski, K. Lips and T. W. Schmidt, Improving the light-harvesting of amorphous silicon solar cells with photochemical upconversion, *Energy Environ. Sci.*, 2012, **5**, 6953–6959.

50 T. F. Schulze, Y. Y. Cheng, B. Fückel, R. W. MacQueen, A. Danos, N. J. L. K. Davis, M. J. Y. Tayebjee, T. Khoury, R. G. C. R. Clady, N. J. Ekins-Daukes, M. J. Crossley, B. Stannowski, K. Lips and T. W. Schmidt, Photochemical Upconversion Enhanced Solar Cells: Effect of a Back Reflector, *Aust. J. Chem.*, 2012, **65**, 480–485.

51 T. F. Schulze, J. Czolk, Y.-Y. Cheng, B. Fuckel, R. W. MacQueen, T. Khoury, M. J. Crossley, B. Stannowski, K. Lips and U. Lemmer, *et al.*, Efficiency enhancement of organic and thin-film silicon solar cells with photochemical upconversion, *J. Phys. Chem. C*, 2012, **116**, 22794–22801.

52 A. Nattestad, Y. Y. Cheng, R. W. MacQueen, T. F. Schulze, F. W. Thompson, A. J. Mozer, B. Fückel, T. Khoury, M. J. Crossley, K. Lips, G. G. Wallace and T. W. Schmidt, Dye-Sensitized Solar Cell with Integrated Triplet–Triplet Annihilation Upconversion System, *J. Phys. Chem. Lett.*, 2013, **4**, 2073–2078.

53 T. F. Schulze, Y. Y. Cheng, T. Khoury, M. J. Crossley, B. Stannowski, K. Lips and T. W. Schmidt, Micro-optical design of photochemical upconverters for thin-film solar cells, *J. Photon. Energy*, 2013, **3**, 034598.

54 Y. Y. Cheng, A. Nattestad, T. F. Schulze, R. W. MacQueen, B. Fuckel, K. Lips, G. G. Wallace, T. Khoury, M. J. Crossley and T. W. Schmidt, Increased upconversion performance for thin film solar cells: a trimolecular composition, *Chem. Sci.*, 2016, **7**, 559–568.

55 S. H. Lee, M. A. Ayer, R. Vadrucci, C. Weder and Y. C. Simon, Light upconversion by triplet-triplet annihilation in diphenylanthracene-based copolymers, *Polym. Chem.*, 2014, **5**, 6898–6904.

56 K. Sripathy, R. W. MacQueen, J. R. Peterson, Y. Y. Cheng, M. Dvorak, D. R. McCamey, N. D. Treat, N. Stingelin and T. W. Schmidt, Highly efficient photochemical upconversion in a quasi-solid organogel, *J. Mater. Chem. C*, 2015, **3**, 616–622.

57 T. Ogawa, N. Yanai, A. Monguzzi and N. Kimizuka, Highly Efficient Photon Upconversion in Self-Assembled Light-Harvesting Molecular Systems, *Sci. Rep.*, 2015, **5**, 10882.

58 J. K. H. Pun, J. K. Gallaher, L. Frazer, S. K. K. Prasad, C. B. Dover, R. W. MacQueen and T. W. Schmidt, TIPSanthracene: a singlet fission or triplet fusion material?, *J. Photonics Energy*, 2018, **8**, 1–9.

59 S. Hoseinkhani, R. Tubino, F. Meinardi and A. Monguzzi, Achieving the photon up-conversion thermodynamic yield upper limit by sensitized triplet–triplet annihilation, *Phys. Chem. Chem. Phys.*, 2015, **17**, 4020–4024.

60 A. Monguzzi, S. M. Borisov, J. Pedrini, I. Klimant, M. Salvalaggio, P. Biagini, F. Melchiorre, C. Lelii and F. Meinardi, Efficient Broadband Triplet–Triplet Annihilation-Assisted Photon Upconversion at Subsolar Irradiance in Fully Organic Systems, *Adv. Funct. Mater.*, 2015, **25**, 5617–5624.

61 A. Monguzzi, D. Braga, M. Gandini, V. C. Holmberg, D. K. Kim, A. Sahu, D. J. Norris and F. Meinardi, Broadband Up-Conversion at Subsolar Irradiance: Triplet–Triplet Annihilation Boosted by Fluorescent Semiconductor Nanocrystals, *Nano Lett.*, 2014, **14**, 6644–6650.

62 L. Frazer, J. K. Gallaher and T. W. Schmidt, Optimizing the Efficiency of Solar Photon Upconversion, *ACS Energy Lett.*, 2017, **2**, 1346–1354.

63 R. B. Piper, M. Yoshida, D. J. Farrell, T. Khoury, M. J. Crossley, T. W. Schmidt, S. A. Haque and N. J. Ekins-Daukes, Kinetic insight into bimolecular upconversion: experiment and simulation, *RSC Adv.*, 2014, **4**, 8059–8063.

64 D. Beery, T. W. Schmidt and K. Hanson, Harnessing Sunlight via Molecular Photon Upconversion, *ACS Appl. Mater. Interfaces*, 2021, **13**(28), 32601–32605.

65 J. E. Yarnell, A. Chakraborty, M. Myahkostupov, K. M. Wright and F. N. Castellano, Long-lived triplet excited state in a platinum(ii) perylene monoimide complex, *Dalton Trans.*, 2018, **47**, 15071–15081.

66 Y. Zhou, F. N. Castellano, T. W. Schmidt and K. Hanson, On the Quantum Yield of Photon Upconversion via Triplet–Triplet Annihilation, *ACS Energy Lett.*, 2020, **5**, 2322–2326.

67 R. W. MacQueen, Y. Y. Cheng, A. N. Danos, K. Lips and T. W. Schmidt, Action spectrum experiment for the measurement of incoherent photon upconversion efficiency under sun-like excitation, *RSC Adv.*, 2014, **4**, 52749–52756.

68 Y. Y. Cheng, B. Fückel, T. Khoury, R. G. C. R. Clady, M. J. Y. Tayebjee, N. J. Ekins-Daukes, M. J. Crossley and T. W. Schmidt, Kinetic Analysis of Photochemical Upconversion by Triplet-Triplet Annihilation: Beyond Any Spin Statistical Limit. The, *J. Phys. Chem. Lett.*, 2010, **1**, 1795–1799.

69 E. M. Gholizadeh, L. Frazer, R. W. MacQueen, J. K. Gallaher and T. W. Schmidt, Photochemical upconversion is suppressed by high concentrations of molecular sensitizers, *Phys. Chem. Chem. Phys.*, 2018, **20**, 19500–19506.

70 A. Haefele, J. Blumhoff, R. S. Khnayzer and F. N. Castellano, Getting to the (Square) Root of the Problem: How to Make Noncoherent Pumped Upconversion Linear. The, *J. Phys. Chem. Lett.*, 2012, **3**, 299–303.

71 A. Monguzzi, J. Mezyk, F. Scotognella, R. Tubino and F. Meinardi, Upconversion-induced fluorescence in multicomponent systems: Steady-state excitation power threshold, *Phys. Rev. B: Condens. Matter Mater. Phys.*, 2008, **78**, 5.

72 J. E. Auckett, Y. Y. Chen, T. Khoury, R. G. C. R. Clady, N. J. Ekins-Daukes, M. J. Crossley and T. W. Schmidt,

Efficient upconversion by triplet-triplet annihilation, *J. Phys.: Conf. Ser.*, 2009, **185**, 012002.

73 M. Kitazawa, T. Yabe, Y. Hirata and T. Okada, Solvent viscosity dependence of bimolecular reaction rate constant of the excited 9-cyanoanthracene quenched by 1,3-cyclohexadiene, *J. Mol. Liq.*, 1995, **65–66**, 321–324.

74 C. Li, C. Koenigsmann, F. Deng, A. Hagstrom, C. A. Schmuttenmaer and J.-H. Kim, Photocurrent Enhancement from Solid-State Triplet–Triplet Annihilation Upconversion of Low-Intensity, Low-Energy Photons, *ACS Photonics*, 2016, **3**, 784–790.

75 A. J. Musser, S. K. Rajendran, K. Georgiou, L. Gai, R. T. Grant, Z. Shen, M. Cavazzini, A. Ruseckas, G. A. Turnbull, I. D. W. Samuel, J. Clark and D. G. Lidzey, Intermolecular states in organic dye dispersions: excimers vs. aggregates, *J. Mater. Chem. C*, 2017, **5**, 8380–8389.

76 R. Vadrucci, C. Weder and Y. C. Simon, Organogels for low-power light upconversion, *Mater. Horiz.*, 2015, **2**, 120–124.